Laser Generated Au–Ag Nanoparticles For Plasmonic Nucleic Acid Sensing

ARTICLE *in* THE JOURNAL OF PHYSICAL CHEMISTRY C · MAY 2012

Impact Factor: 4.77 · DOI: 10.1021/jp301735c

THE JOURNAL OF PHYSICAL CHEMISTRY C

Article

pubs.acs.org/JPCC

Laser-Generated Au–Ag Nanoparticles For Plasmonic Nucleic Acid Sensing

Anne-Marie Dallaire,[†] David Rioux,[†] Alexandre Rachkov,[‡] Sergiy Patskovsky,[†] and Michel Meunier*[,†]

[†]Department of Engineering Physics, Laser Processing and Plasmonics Laboratories, École Polytechnique de Montréal, C. P. 6079, succ.Centre-Ville, Montréal (Québec), Canada, H3C 3A7

[‡]Institute of Molecular Biology and Genetics of National Academy of Sciences of Ukraine, 150 Academician Zabolotny Street, Kyiv, Ukraine, 03143

ABSTRACT: The development of nanoplasmonic sensing approaches for DNA detection based on the localized plasmonic properties of different metallic NPs fabricated by femtosecond laser ablation with an application for synthetic oligonucleotides as specific probes for genetic sequence variations is presented. The planar surface plasmon resonance (SPR) technique has been used to test oligonucleotide probes specific to *rpoB* genes of *Mycobacterium tuberculosis*. Optimal experimental conditions providing efficiency of hybridization between immobilized probe and cDNA target and performance of the SPR method were obtained and applied to the nanoplasmonic biosensing based on colloidal nanoparticles. Gold and silver/gold alloy nanoparticles were fabricated by the "pure" laser ablation method and have shown faster conjugation to thiol-modified DNA and higher stability in hybridization buffer than nanoparticles produced by chemical synthesis. Nanoparticle-enhanced and spectral SPR methods were used to confirm the efficiency of DNA-modified laser-generated gold nanoparticles in biosensing. Numerical estimation shows a higher sensitivity of nanoalloy materials application in dimer aggregate configurations. The described approaches could be proposed as a basis for an optical biosensor for sensitive and real-time detection of nucleic acid samples, for example, nucleotide sequences related to drug-resistant tuberculosis.

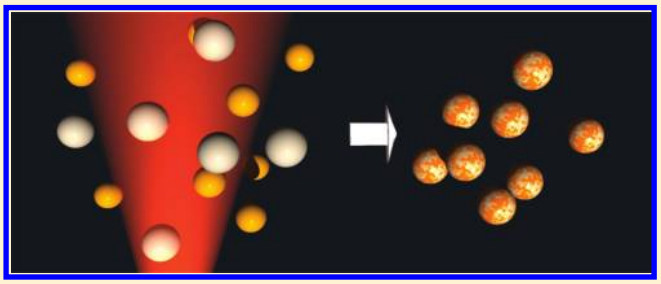

1. INTRODUCTION

Despite the importance of accurate and rapid diagnosis and recent developments of powerful methods, such as PCR and ELISA, routine diagnostics of many infectious diseases (including tuberculosis) is still slow and has a poor detection threshold and limited ability to differentiate between multiple pathogens. The ideal diagnostic device would need to be a cost-effective, portable, and point-of-source or point-of-care detection system that would be highly sensitive and accurate and that could differentiate multiple pathogens. A number of these detection problems could be overcome by using nanoplasmonic technology. Although it is still in an experimental stage, nanoplasmonics has the potential to be used in future applications as extremely sensitive biomolecular sensors. Colloidal plasmonic materials, such as gold, alloys, or nanoshell nanoparticles (NPs), have shown promising results when used as optical markers on bacteria, cells, or DNA.[1,2]

Gold nanoparticles exhibit a typical LSPR band centered at around 520 nm that can be easily synthesized via reduction of a gold salt. These materials are widely used in the development of methods for specific DNA detection via functionalization by thiol-modified oligonucleotides.[3−5,9] The extinction coefficient of the surface plasmon band for a Ag particle (between 390 and 420 nm depending on the particle size) is approximately 4 times as large as that for a Au particle of the same size.[6−8] However, the synthesis of AgNPs with a homogeneous size distribution is considerably more difficult than that of AuNPs, and the efficiency of thiol functionalization is significantly lower. Gold–silver NPs were first synthesized in an effort to combine the optical properties of silver with the affinity of gold to bind to sulfur atoms.[12] Cao et al. first described the application of bimetallic NPs composed of a silver core and a gold shell (Ag/Au) and functionalized by thiol-modified oligonucleotides for identification of nucleotide sequences.[10,11] Alloy nanoparticles, unlike their core–shell counterparts, can be synthesized using the same reducing agent, in a much simpler and rapid process.[8,12] An alternative method to obtain bioconjugated gold or alloy nanoparticles in a one-step process without the need of chemical precursors and reducing agents is laser ablation in liquids.[13−15] This modern nanofabrication technology allows the synthesis of colloidal plasmonic materials in the selected liquid medium with a controlled surface chemistry adapted for the best performance in volume biosensing or surface modification.[17]

This work is aimed at the development of nanoplasmonic sensing approaches for DNA detection based on the localized plasmonic properties of different metallic NPs fabricated by femtosecond laser ablation with an application of synthetic

Received: February 22, 2012
Revised: April 26, 2012
Published: April 30, 2012

oligonucleotides as specific probes for genetic sequence variations.[16]

To determine the optimal parameters for plasmonic biosensing of our specific DNA sequence, namely, the hybridization buffer concentration, the experiment was first conducted on a conventional planar SPR system. These parameters were then transferred to the colloidal nanoplasmonic sensing taking into account the difference between volume and surface biosensing geometries. We think that this approach is very important and efficient when the possibility exists to apply a well-established methodology, such as the conventional SPR method, to find and verify the optimal experimental protocol for the sensing methods based on a similar physical phenomenon. We compared laser-generated gold and silver/gold alloy NPs with chemically produced NPs in terms of their optical resonance properties and of their stability in an optimal concentration of saline−sodium citrate hybridization buffer (SSC buffer). The described approaches are meant to be a first step toward the development of an innovative technique for fast and sensitive detection methods based on the hybridization of complementary or mismatched oligonucleotides.

2. MATERIALS AND METHODS

2.1. Reagents. The single-stranded oligonucleotides were synthesized by Integrated DNA Technologies (IDT,Germany). Urea and KH_2PO_4 were purchased from Fluka (Buchs, Switzerland). 6-Mercapto-1-hexanol (MCH) and SSC buffer 20× concentrate (0.3 mM sodium citrate, 3 M NaCl, pH 7) were obtained from Sigma (Oakville, Canada). All solutions were made with deionized Milli-Q water. The 20 nm citrate-coated gold NPs produced by chemical reduction methods were purchased from (Sigma-Aldrich, USA). These NPs will be referred to in the text as Sigma-NPs.

Gold and silver/gold alloy NPs were synthesized by femtosecond laser ablation either in deionized water, oligonucleotide solution, or oligonucleotide + SSC buffer solution. The advantage of the laser ablation synthesis method is the possibility to produce ultrapure NPs in any liquid, including pure deionized water without using reducing agents and other chemicals as surfactants. Solutions could also be a very low sodium citrate concentration or NaOH, impossible to use in the production of stable NPs by conventional chemistry. It is also possible to functionalize the surface during or immediately after the ablation. To produce gold NPs, a gold target (Alfa Aesar, USA) was placed at the bottom of a glass cuvette filled with 1 mL of liquid. The liquid height over the target was about 1 mm. The laser beam from a Ti:sapphire amplifier (Spectra-Physics, Spitfire Pro, 1 kHz rep rate, 40 fs fwhm pulse duration) was focused on the gold target using a 75 mm focal length lens. The laser spot on the surface of the gold target was about 0.5 mm in diameter. The laser beam with an energy of about 500 μJ/pulse was scanned over the target surface at a constant speed of 0.5 mm/s for 5 min. The ablation process resulted in a colloidal suspension of NPs with a bright red coloration, indicating small nonagglomerated particles. These NPs will be referred to as LA-GNPs (for laser ablated gold nanoparticles, to indicate that they were generated by laser ablation). The same process was used for silver NPs, resulting in a yellow solution. To fabricate alloy nanomaterials (LA-ANPs), small aliquots of gold and silver NPs solutions were mixed in a 8 mL glass vessel in the right proportion to obtain the desired gold-to-silver ratio. The femtosecond laser beam was then focused from the side into the solution in order to induce alloying of the silver and gold particles. The solution is continuously mixed during the alloying process, which goes on for about 2 h in order to ensure homogeneity of the particle composition. This process resulted in a stable solution of the alloy nanoparticles[18] with different shades of orange depending on the gold-to-silver ratio.

Extinction spectra of colloidal NPs were measured with a portable spectrometer (Ocean Optics, USB4000-UV/vis) or with a VASE spectroscopic ellipsometer (J. A. Woollam Co). To obtain the NP concentration, quasi-static approximation and Mie theory were used to determine the size-dependent extinction coefficients, and these were compared with measured extinction spectra. TEM was used to measure the particle size distribution, and a mean diameter of about 20 nm was found for the gold and alloy samples. Concentrations of the LA-GNPs and LA-ANPs solutions were matched to the concentration of the Sigma colloidal solution.

2.2. Selection of Oligonucleotide Sequences. Resistance to refampin and related rifamycins is known to arise as a result of mutations occurring in a discrete region of the *rpoB* gene of *M. tuberculosis* that alters the sequence of a 27 amino acid region of the RNA polymerase β subunit.[19,20] Therefore, we decided to use this hot spot of the *rpoB* gene. The selection of the length and the sequence of the oligonucleotide probe was made based on its ability to form intramolecular and intermolecular interactions because the formation of strong secondary structures within the potential probe could be an obstacle for the efficient hybridization with complementary targets in the analyzed solutions. As a probe, among the oligonucleotides possessing the lowest ability to intramolecular interactions, we have chosen the 21-mer ACCCA-CAAGCGCCGACTGTTG from the *rpoB* gene of *M. tuberculosis*, which contains the mutated TCG → TTG codon 531 associated with rifampin-resistant tuberculosis, and have named it P2. For immobilization on a gold surface of the sensor chip, the 5′-end of the oligonucleotide was modified by an SH group via a spacer of six methylene groups. This spacer is necessary to decrease the probability of steric hindrances for hybridization near the sensor surface. For hybridization selectivity testing, the following target oligonucleotides were used: T2 (CAA-CAGTCGGCGCTTGTGGGT), complementary to P2; T2mod, oligonucleotide T2 that was modified by an SH group; TN (CGACAGTCGGCGCTTGTGGGT), containing a single-base mismatch (complementary to the sequence containing normal TCG codon 531 of the *rpoB* gene).[21] The calculated free energy changes (using DINAMelt Web server[22]) of their self-hybridization showed that formation of a stable internal secondary structure of these oligonucleotides is hardly probable.

2.3. SPR System Setup. A homemade planar SPR system was developed to evaluate the optimal conditions for hybridization of the selected oligonucleotides. It was used to estimate the dynamic characteristics of attachments and the concentration and surface coverage by DNA and to obtain the sensitivity limit of the plasmonic sensing method. A schematic diagram of the instrument design is shown in Figure 1. A 5 mW superluminescent light-emitting diode (SLED) (QPhotonics) operating at a wavelength of 680 nm with a 10 nm bandwidth was used as the light source. Optical filtering is applied to produce a uniform convergent beam, and a polarizer is used to set the linear p-polarization. The SPR sensor system includes a glass coupling prism (60° BK7). A homemade or commercial

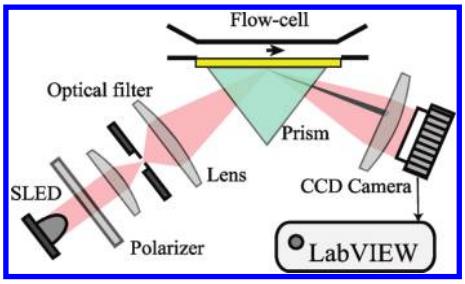

Figure 1. Experimental CCD camera based SPR setup.

biosensor chip (Biacore, Platypus) with a 50 nm gold thin film was then placed in immersion contact with the prism. For the real-time tests, a flow injection measuring cell with a volume of 6 μL was designed. The entire system was placed on a rotating stage with a possibility of 2-D linear translation for exact beam positioning. The stability and low coherence of the light source greatly improve the image of the SPR peak recorded by the linear CCD camera (Ames Photonics Inc., Hurst, TX). Software for signal acquisition and treatment was developed on LabView. For numerical analysis of the obtained SPR curves, a polynomial curve fitting method of the third order was used. Primary SPR response values were expressed in arbitrary units where 1 a.u. is equal to the 1 pixel shift on the CCD camera that corresponds to the 3.6×10^{-3}° of angular shift or 2.12×10^{-5} RIU for the BK7 prism. The estimated noise level was about 0.2 pixels and corresponds to a sensitivity limit of 4.3×10^{-6} RIU. Prior to modification, the gold surface of the glass slides was cleaned with freshly prepared "piranha" solution (3:1 mixture of concentrated H_2SO_4 and 30% H_2O_2) at room temperature for 2 min, then rinsed thoroughly with Milli-Q water, and dried in a nitrogen flow. The cleaned gold slide was placed on the SPR coupling prism using a refractive index matching immersion liquid (Cargille Laboratories, USA). The flow rate (50 μL/min) was controlled by a peristaltic pump "Ismatec" (IDEX Corporation, Switzerland).

3. RESULTS AND DISCUSSION

3.1. Optimization of Reaction Conditions: Efficiency of Hybridization for P2−T2. DNA hybridization sensor performance is related to its ability to recognize nucleic acid molecules contained in analyzed samples by surface-bound capture probes. However, the hybridization and its efficiency over solid supports depend on many parameters and phenomena, such as the analyte diffusion toward the surface of the sensor, its bidimensional diffusion, the adsorption and desorption, the size of probes and targets, the target concentrations, and surface probe densities.[23] Whereas hybridization on a sensor surface was reported to be successful under various conditions, molecular biology literature[24] recommends the usage of SSC buffer solution, for example, 6 × SSC buffer solution for oligonucleotides hybridization, and 2 × SSC buffer solution for washing out nonspecifically adsorbed nucleic acids after hybridization. Indeed, the ionic strength of the hybridization buffer strongly influences the hybridization of DNA sequences as well as the sensitivity of the plasmonic sensors to the recognition of the surface thin biofilm formation. Figure 2a presents the calculated values of free energy changes for hybridization in solution between the studied oligonucleotides at various concentrations of SSC buffer solutions (calculated using DINAMelt Web server[22]). As it was expected, an increase in ionic strength leads to strengthening of intermolecular interactions that can be explained by shielding of negatively charged phosphate residues by counterions of the buffer solution and, consequently, creating more favorable conditions for hydrogen binding between complementary nucleic bases, thus resulting in a more sensitive biosensing. The increase in ionic strength leads to a drastic increase in the interaction strength up to approximately 2 × SSC; then, further changes become less pronounced.

On the other hand, increasing buffer concentration leads to an increase of working medium refractive index (RI) and, consequently to a decrease in plasmonic sensor efficiency. We have numerically modeled SPR sensor sensitivity with angular and spectral interrogation methods to the surface thin film forming with a thickness equal to the length of the P2−T2 duplex. Using ref 25, we can estimate the length of ssDNA P2 to be 13 nm with 0.63 nm/nucleotide while creation of dsDNA P2−T2 leads to a length shortening, resulting in a total length of 7 nm with 0.34 nm/nucleotide. The experimentally determined RI of SSC buffers with different concentrations

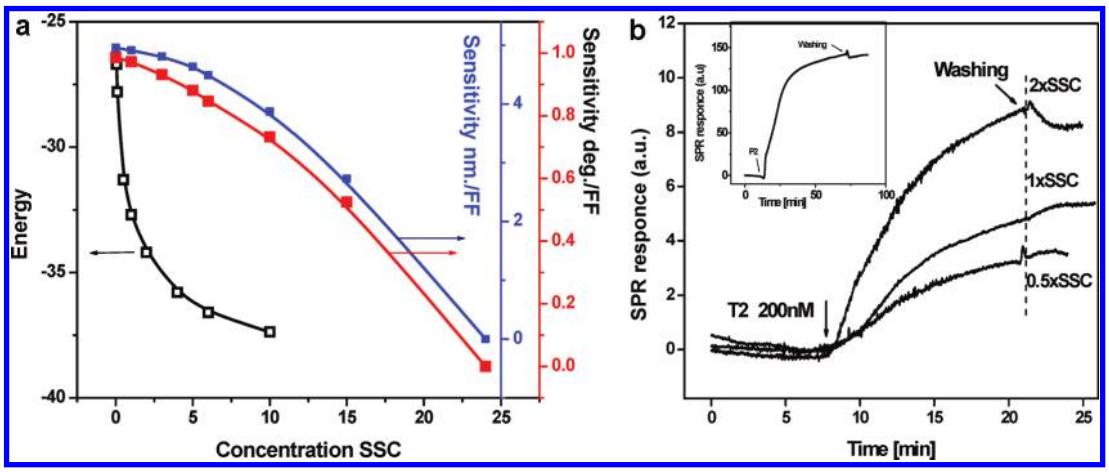

Figure 2. (a) Free energy changes (kcal/mol) associated with hybridization between probe and target for different concentrations of buffer SSC and calculated SPR sensitivity for 7 nm thin biofilm with RI = 1.530. (b) SPR response for comparison of the efficiency of P2−T2 hybridization under indicated different concentrations of buffer SSC with 200 nM T2 concentration. (b, inset) SPR response for covalent immobilization of thiol-modified P2 on the gold surface.

dx.doi.org/10.1021/jp301735c | J. Phys. Chem. C 2012, 116, 11370−11377

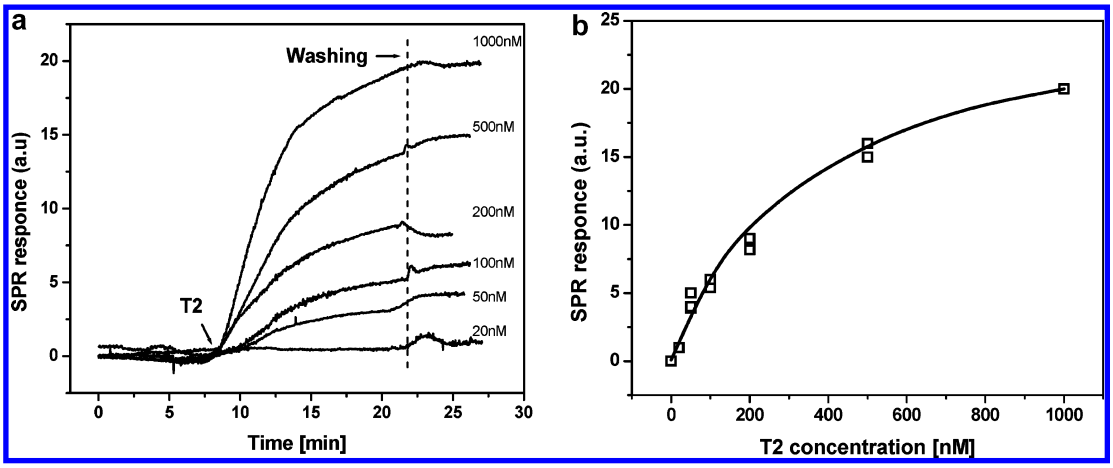

Figure 3. (a) SPR response for hybridization between the surface-bound capture probe P2 and the complementary target T2 at various concentrations. (b) Dependence of SPR response as a function of T2 concentration in 2 × SSC.

was used as a working medium. Maxwell−Garnet effective medium theory[26] and a refractive index equal to 1.456 for ssDNA and 1.530 for dsDNA[27] were used to estimate the RI of the surface biofilm. The calculated SPR response shows linear dependences for angular and spectral shift on the surface thin film filling factor (FF). The line slope at different buffer concentrations is used to estimate sensitivity, as presented in Figure 2a. In the range up to approximately 5 × SSC, the decrease in the SPR sensitivity is minimal. Therefore, the 2 × SSC buffer concentration was considered as optimal in order to provide efficient hybridization between oligonucleotides at conditions where high SPR sensor sensitivity is still preserved.

To evaluate the best experimental conditions for hybridization of the specific probe and selected target and to confirm our theoretical predictions, several calibration tests were performed on the developed planar SPR system. Immobilization of thiol-modified capture probes on the gold sensor was carried out in the immobilization solution (0.5 M KH_2PO_4, pH 3.8). Before the probe immobilization, a stable baseline was obtained by pumping the solution through the measuring cell at the flow rate of 50 μL/min, at room temperature. A 1 μM portion of the thiol-modified probe P2 in the same immobilization solution was then pumped during 20 min. The flow was stopped for 40 min incubation. The measuring cell was then washed by the immobilization solution until a stable sensor signal is obtained.

Efficient immobilization of the 1 μM of probe P2 on the gold surface was detected by the SPR system (Figure 2b, inset). When completely stretched, the 21-mer oligonucleotide is about 13 nm in length, but in buffer solution, the real geometry is more complicated and the effective total film thickness is estimated at 9 nm.[28,29] Including this effect in our calculation, we obtained a filling factor of the thin surface DNA biofilm of about 20%.[30] These concentrations could be considered optimal because, if the filling factor is too high, the close proximity of the P2 probes prevents the passage of the T2 complementary oligonucleotide, lowering the hybridization rate.[31] After the P2 immobilization stage, to prevent interactions of DNA from the analyzed sample with the gold surface, the sites on the gold surface free from thiol-modified oligonucleotides were blocked by the 1 mM aqueous solution of mercapto-hexanol (MCH). Figure 2b presents experimental SPR results on the efficiency of 200 nM T2 hybridization at different buffer SSC concentrations, which confirm higher responses with increasing buffer concentration. When looking for the optimal experimental conditions, another aspect of high buffer concentration, such as its influence on the colloidal NPs' stability, should also be considered.[3] Therefore, even if a higher buffer concentration could further improve the hybridization efficiency and plasmonic sensor response, experimental application of nanomaterials or hybrid nanoplasmonic schemes will be complicated. In our case, the best compromise between efficient hybridization of the selected probe and target, sensitivity of the plasmonic planar sensor, and stability of the NPs is a buffer concentration of 2 × SSC. Moreover, the neutral pH of this buffer will have a negligible effect on the SPR sensitivity and stability of the colloidal NPs.[32]

To investigate the parameters and limitation of the plasmonic biosensing scheme based on hybridization between oligonucleotides P2 and the complementary target T2, we have performed experimental tests using the planar SPR system. Real-time results of P2−T2 hybridization at various T2 concentrations are presented in Figure 3a. We used a 2 × SSC running buffer concentration for the stage of hybridization and chose a hybridization time of 3 min for sample injection and 10 min for incubation at stopped flow. After that, the measuring flow cell was washed by injecting buffer solution at a standard flow rate (50 μL/min). For regeneration of the bioselective element, 8 M urea is used. As follows from the calibration curve presented in Figure 3b and the optical setup noise limits (0.2 a.u.), our SPR system could detect up to 6 nM T2 oligonucleotide and saturates slightly above 1 μM.

3.2. Laser-Generated NPs for Oligonucleotide-Based Biosensing. In this work, we are considering application of gold and gold/silver alloy NPs for oligonucleotide-based biosensing. We believe that novel colloidal plasmonic materials with unique localized optical properties can allow the development of novel promising biosensing designs and architectures, impossible to achieve with conventional planar SPR technology. Moreover, femtosecond laser ablation nanofabrication technology provides the possibility to produce complex plasmonic nanomaterials in a controlled medium with specific optical properties, thereby simplifying sensitive volume biosensing.

To maximize sensor response and maintain good efficiency of hybridization between the chosen probe and target, the NPs have to be stable in the aforementioned 2 × SSC target buffer concentration. First, we tested stability in this buffer solution

dx.doi.org/10.1021/jp301735c | J. Phys. Chem. C 2012, 116, 11370−11377

for laser-generated NPs (LA-GNPs and LA-ANPs) and for unmodified Sigma-NPs.

Spectral analysis of localized plasmon shows that the unmodified NPs are very unstable even in a low SSC buffer concentration. For all types of particles studied, we observed a rapid agglomeration for a 0.2 × SSC buffer concentration (Figure 4). The decrease of the peaks at 520 nm (Au NPs) and

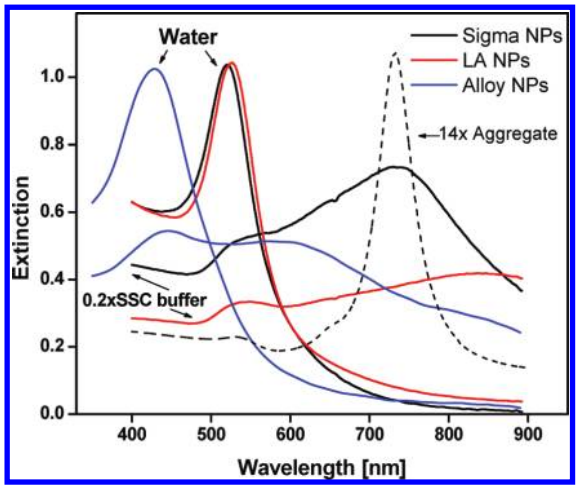

Figure 4. Agglomeration of the NPs in deionized water and in 0.2 × SSC buffer solution. Simulation of the aggregated spectrum for LA-NPs is presented by the dashed line.

425 nm (alloy NPs) and the appearance of a wide peak shifted to the NIR are a strong indication of agglomeration in the NP solution. LA-NPs show a more rapid and pronounced aggregation than Sigma-NPs in the ionic environment, which is expected from the absence of a stabilizing agent on LA-NPs. Performed calculations using generalized multiparticle Mie-solution (GMM)[33] for the linear array of closely packed 20 nm NPs show a similar peak around 733 nm, confirming the formation of aggregates of at least 14 NPs (Figure 4, dashed line).

We expect that thiol-modified DNA strands attached on the surface of a gold NP will act as a stabilizing agent and prevent the agglomeration of the NPs by electrostatic and steric repulsion.[34] Gold particles are quite easy to modify because they are often stabilized with a weakly binding layer of charged ligands (e.g., citrate) that can be replaced with molecules with chemical functionalities that bind more strongly (e.g., thiols) to their surfaces than these ligands. However, the standard DNA attachment procedure on gold NPs with the so-named salt-aging process requires many days.[3] In 2006, functional modifications have been made to the procedure: the final salt concentration of the solution is reached within several hours, as opposed to 40 h, as originally described.[35,36] This "fast" salt aging is made possible by the addition of surfactant molecules prior to salt aging. During this "fast" salt aging, the concentration of NaCl was increased to 0.05 M using 2 M NaCl; then this process was repeated at one more increment of 0.05 M NaCl and for every 0.1 M NaCl increment thereafter until a concentration of 1.0 M NaCl was reached. The salting process was followed by incubation overnight at room temperature. This rather cumbersome process is made possible by the addition of surfactant molecules and maintaining an SDS concentration at every salt addition. We want to investigate the possibility of a quite simple, one-step immobilization procedure with the use of the same buffer solution (SSC) at first for nanoparticle modification and then during further hybridization of the attached oligonucleotides with complementary sequences.

To test the influence of DNA modification on the stabilization of colloidal NPs, we measured spectral properties of colloidal solutions during formation of the DNA−Au NPs complex. The idea is to add oligonucleotides to the freshly ablated NPs solution and then to test the NPs' stability in SSC buffer after different times of DNA attachment. Gold and alloy NPs were produced in deionized water and showed an original narrow extinction peak around 523 and 425 nm, correspondingly. TEM imaging and Mie theory calculation show NPs sizes around 20 nm in diameter. One minute after ablation, we added thiolated oligonucleotides with a concentration of 2 μM. For comparison, a similar procedure was performed with Sigma-NPs. After 10 min, 30 min, and 16 h of incubation time, we measured the extinction spectrum of each NP solution in different SSC buffer concentrations, and the last test was done after 24 h to estimate the long time stability.

As an example, results for NP stability after 10 min of incubation are presented in Figure 5a−c. The Sigma-NPs begin to agglomerate at 0.33 × SSC and show formation of clusters composed of about seven NPs. In 0.5 × SSC buffer concentration, our calculations confirm the dominant existence of 12 × nanoaggregates, and this solution is also unstable after 24 h. Such behavior is very close to that of the unmodified NPs. However, for the freshly ablated LA-GNPs, agglomeration is much weaker even at 0.5 × SSC. They remain relatively stable at 1 × SSC. Some aggregates are formed, but the peak at 520 nm is still clearly visible, indicating that a good fraction of nonagglomerated particles is still present even after 24 h. Similar stability was demonstrated by LA-ANPs with aggregate formation that begins at 0.5 × SSC buffer concentration. As a parameter responsible for NP stability, we choose normalized extinction dependence on the buffer concentration for different incubation times of T2mod (2 μM) at 520 nm for gold NPs and 425 nm for the alloy (Figure 5d). As follows from the obtained results, after 30 min incubation time, LA-GNPs can withstand 0.66 × SSC much better than the Sigma-NPs after 16 h incubation. After 16 h incubation, LA-NPs do not agglomerate significantly up to 1.33 × SSC. These results suggest that, after 16 h incubation time, enough oligonucleotides have attached to LA-GNPs to ensure their stability in the buffer solution. Even better, if we are willing to use a lower SSC concentration, the LA-NPs can be used up to 0.66 × SSC with only 30 min incubation time. After a gentle centrifugation to wash off the remaining unattached oligonucleotides, these NPs could be used directly in SPR tests. In comparison, the normal attachment procedure for chemically produced NPs requires 16 h incubation, a 40 h salt aging process, and long cleaning steps before the NPs are stable enough to be useable for SPR tests. Interesting results were obtained for LA-ANPs: after 10 and 30 min of incubation, results were similar to the LA-GNPs, but 16 h modification show a nonlinear behavior with high stability up to 1.33 × SSC and a rather sharp drop at 2 × SSC.

We conclude that oligonucleotides attach more easily to freshly ablated gold and alloy NPs than to Sigma-NPs. We believe that this difference could be explained by the absence of a stabilizing agent on LA-NPs, as opposed to citrate-coated Sigma-NPs. Indeed, adsorption kinetics of a negatively charged thiol ligand to gold NPs is known to be determined by the desorption of the outgoing ligand step.[37,38]

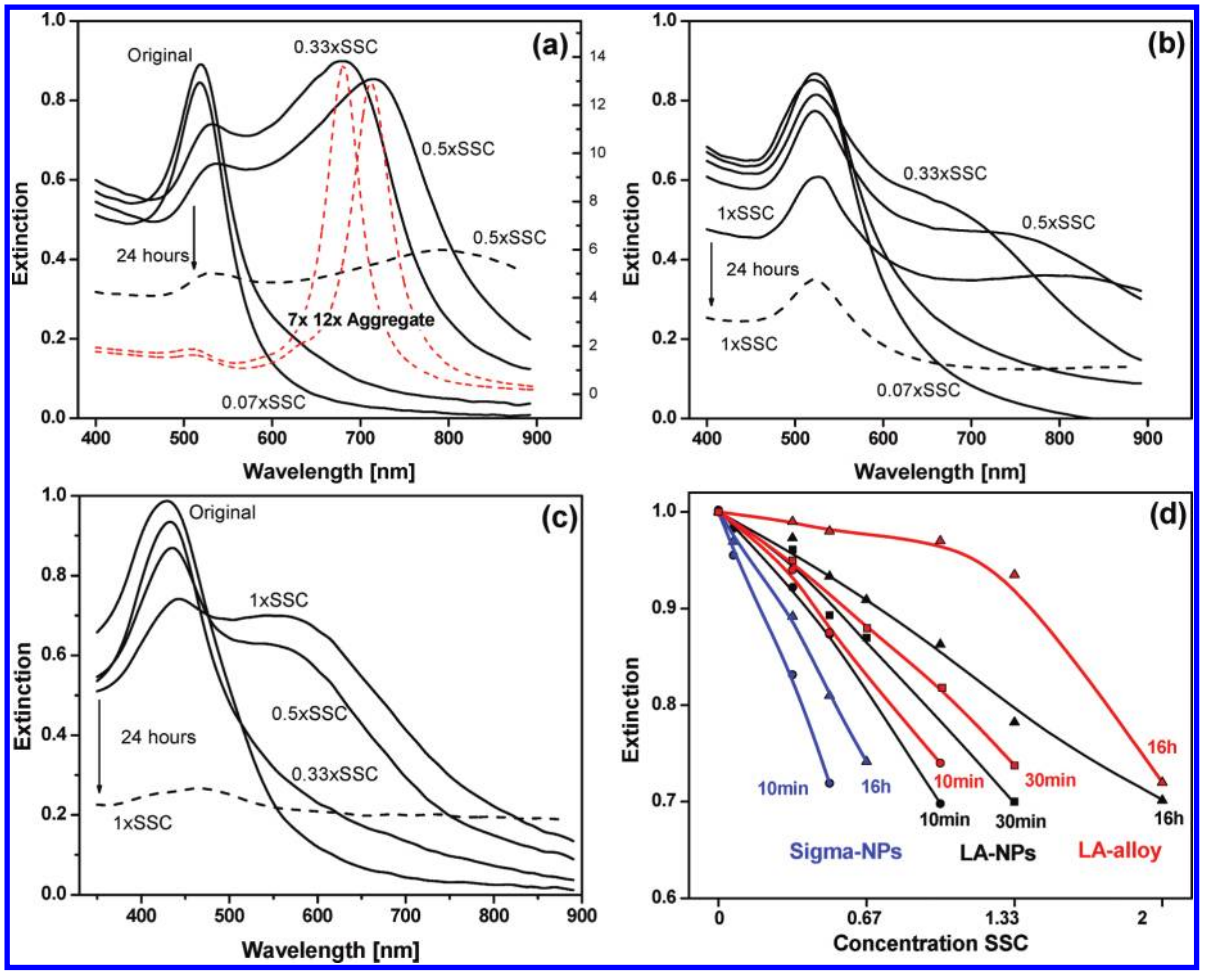

Figure 5. Extinction spectra of Sigma-NPs (a), LA-GNPs (b), and LA-ANPs (c) with increasing concentration of SSC buffer for 10 min incubation with T2mod (2 μM). (d) Extinction dependence on the buffer concentration for different incubation times of T2mod (2 μM) at 520 nm for Sigma-NPs and LA-GNPs and 425 nm for LA-ANPs.

Stability of the modified NPs could also be improved by increasing the concentration of the T2mod oligonucleotide, as is shown in Figure 6. The NP concentration dependence calculated from the experimental spectral data is shown in the inset of Figure 6. For example, for 1 μM T2mod, the final NP concentration at 2 × SSC is 2 × 10^{11} NPs/mL, whereas for 2 μM T2mod, it is 3 × 10^{11} NPs/mL. By using parameters of the oligonucleotides,[39] we have verified that the surface is still not saturated at a 2 μM concentration. Also, any nanoplasmonic sensing that uses resonance NP properties depends on the quality of the spectral curves, namely, its contrast and half-width. As can be concluded from Figure 6, a small concentration change results in much higher changes in the signal-to-noise ratio.

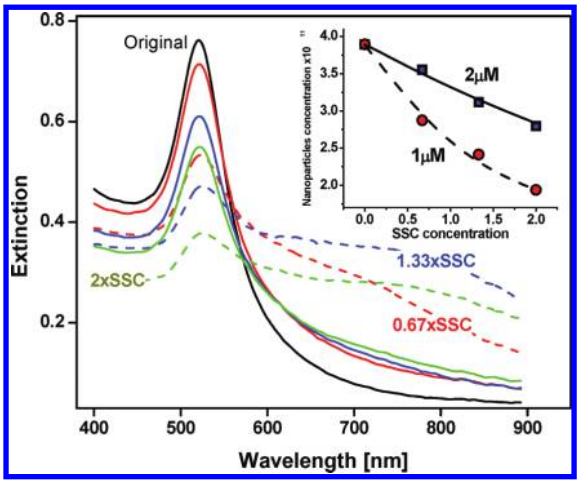

Figure 6. Extinction spectra of LA-NPs with increasing concentration of salt for 1 μM (dashed line) and 2 μM (solid line) T2mod (16 h incubation; red lines, 0.67 × SSC; blue lines, 1.33 × SSC; green lines, 2 × SSC). Inset: NP concentration dependence on buffer concentration.

We also performed the laser ablation directly in a 2 mM oligonucleotide solution in 2 × SSC buffer concentration. The extinction spectrum showed a wide peak around 520 nm, indicating the presence of small nonagglomerated particles. An additional extinction peak at higher wavelengths confirms that aggregated NPs are also present in the solution. As a conclusion, even in the presence of highly concentrated SSC buffer, some of the oligonucleotides attach quickly enough on the NPs so that they partly prevent their agglomeration. Furthermore, since we already have particles in 2 × SSC, we could simply wait for the agglomerated fraction to precipitate, or gently centrifuge the solution in order to remove the agglomerates.

3.3. Two Approaches to NP-Mediated DNA Detection.

Our previous results show that thiol-modified oligonucleotides

dx.doi.org/10.1021/jp301735c | J. Phys. Chem. C 2012, 116, 11370−11377

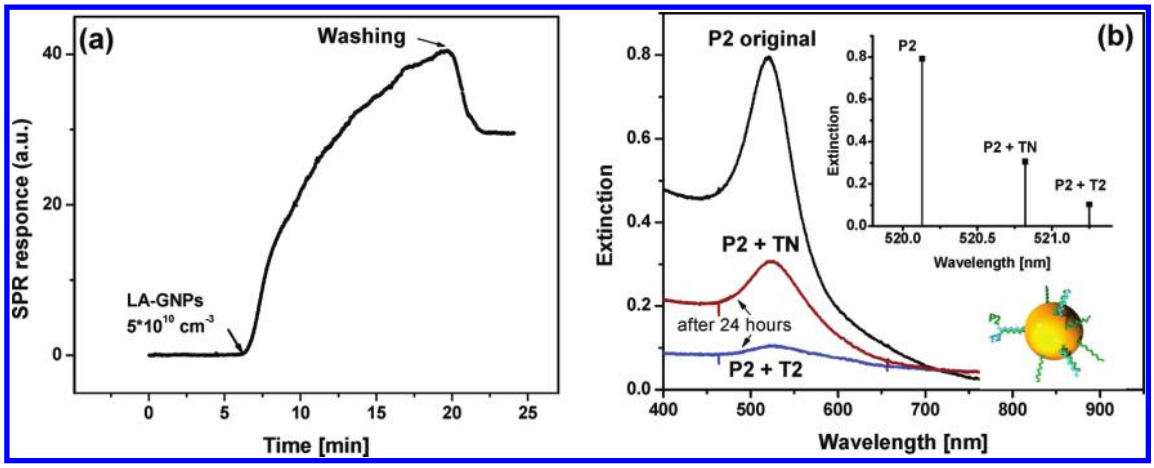

Figure 7. (a) Test of NP-enhanced planar SPR biosensing and direct T2mod hybridization. (b) Extinction spectra for LA-GNPs modified by P2 after hybridization with complementary T2 and one-base mismatch TN oligonucleotides in 1 × SSC after 24 h. Inset: amplitude and spectral shift after hybridization.

have successfully attached to LA-NPs to form a stable complex in 2 × SSC buffer solution. We now want to investigate the possible uses of these NP-modified oligonucleotides in different nucleic acid biosensing schemes and confirm that they are active and able to hybridize selectively. In this article, two experimental approaches for LA-GNP-mediated DNA detection were tested: NP-enhanced planar SPR detection and application of spectral properties of localized surface plasmon for biosensing in volume. As a way to increase the sensitivity of the volume sensing, we also considered theoretically the plasmonic spectral response for sensors based on formation or destruction of nanodimers formed by gold or alloy NPs.

For the NPs-enhanced planar SPR approach, LA-GNPs modified by T2mod during 30 min were cleaned by centrifugation (three times for 5 min), and a concentration of about 5×10^{10} cm^{-3} was measured from the extinction curve. The real-time dynamics of T2mod-LA-GNPs attachment to P2 attached on the gold surface of the SPR sensing block was detected in 1 × SSC buffer (Figure 7a). A similar test with unmodified planar gold did not show a considerable response, strongly suggesting that the DNA:LA-GNPs complexes have successfully hybridized with the surface immobilized probe and, therefore, are suitable for NP-mediated sensing. Using the Maxwell−Garnett effective medium approximation for the thin film with a thickness that corresponds to the gold NP's diameter (20 nm) with 7 nm of dsDNA as surface modification, we have estimated the surface NP concentration to be around 1.7×10^9 particles/cm^2. Considering the ideal case where each of these nanoparticles is attached to only one oligonucleotide and that all of them are detected on the surface, a sensitivity of 0.3 fM was estimated, which is much better than the 6 nM for theunmodified target. However, for real application, the sandwich hybridization method will be developed.

The second approach is to use spectral properties of the localized surface plasmon of LA-GNPs for biosensing in volume. Here, 1 mL of freshly laser-ablated NP solution was modified by 1 μM of P2 oligonucleotides. Spectral tests for hybridization with 1 μM of complementary T2 and one-base mismatch TN oligonucleotides in 1 × SSC were then performed. No immediate change was detected. After 24 h of hybridization, the spectral measurements were repeated (Figure 7b). In the inset in Figure 7b, the extinction peak amplitude and wavelength position for the P2-LA-GNPs original solution and P2−T2 and P2−TN complexes are shown. We estimated the changes in gold NPs' surface modification using exact Mie calculations for nanoshell structures. Results show that a spectral shift of 0.69 nm for the P2−TN complex correspond to a 15% change in surface filling factor for 7 nm thin film. For the P2−T2 complex, we obtained a 1.12 nm shift that corresponds to a 21% surface change. The P2−T2 complex shows a lower stability at this buffer concentration, but a higher spectral response than the P2−TN complex. The obtained results require a future investigation but already show a possible methodology for the DNA test and also for discrimination of single-base mismatch oligonucleotides and can be proposed as a basis for an optical biosensor for detecting single-stranded oligonucleotides related to the *rpoB gene of Mycobacterium tuberculosis*.

Spectral biosensing after NP modification with 21-mer oligonucleotides is quite limited due to the low resulting shift (inset in Figure 7b). To improve sensitivity, we want to consider sensor design where NP dimer formation is used as a sensible parameter.[40] Here, we see the great potential of Au/Ag alloy particles fabricated by the laser ablation method. Using Mie calculation for spherical aggregates and dielectric function from ref 41, we have estimated the spectral response of alloy dimers with different diameters and with a 7 nm interparticle distance equal to the P2−T2 complex (Figure 8). Results demonstrate that using larger NPs increases the spectral shift, but the extinction peak becomes larger, thus complicating the determination of the initial and final maximum extinction positions. For 20−40 nm particles, the sensitivity could be improved more than 2 times by employing, for example, a 67% Ag/33%Au nanoalloy.

The presented preliminary results show the great potential of LA-NPs application for enhanced plasmonic detection of nucleic acid samples.

4. CONCLUSIONS

In this work, we investigated the possibility to use gold and alloy NPs fabricated by femtosecond laser ablation technology in different plasmonic biosensing setups for detection of single-stranded oligonucleotides. To confirm the activity of DNA surface immobilization, we have performed preliminary tests of two experimental approaches for LA-GNP-mediated DNA detection. We also discussed theoretically the possibility of the

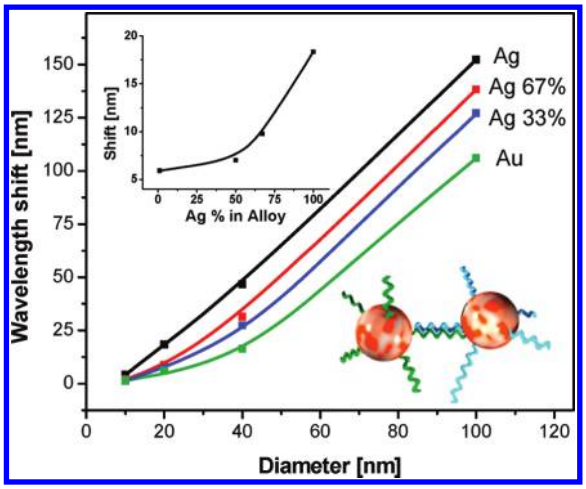

Figure 8. Calculated spectral shift of maximum extinction position as a function of NP size for dimer formation with an interparticle distance of 7 nm. Gold, silver, and alloy particles are shown. Inset: calculated shift for nanoalloy dimers with a 20 nm particle diameter.

nanoparticle-based method sensitivity improvement. Optimal reaction conditions and efficiency of hybridization between the immobilized probe on the gold surface and the cDNA target was tested by the planar SPR system, and the sensitivity limit was determined. A buffer concentration of 2 × SSC is the best compromise between hybridization rate, plasmonic sensor sensitivity, and stability of colloidal NPs. We have also shown that thiol-modified oligonucleotides attach more easily to laser-generated gold NPs than to Sigma-NPs produced by chemical reduction. DNA-modified laser-generated NPs are thus more stable in the buffer solution and better suited for SPR experiments. Furthermore, their production requires much fewer steps than the standard salt aging process and can be functionalized much faster.

AUTHOR INFORMATION

Corresponding Author

*E-mail: michel.meunier@polymtl.ca.

Notes

The authors declare no competing financial interest.

ACKNOWLEDGMENTS

The authors acknowledge the financial contribution from the Natural Science and Engineering Research Council of Canada, and from Strategic Network for Bioplasmonic Systems (Biopsys).

REFERENCES

(1) Hartland, G. V.; Schatz, G. C. *J. Phys. Chem. C* **2011**, *115*, 15121−15123.
(2) Schwartzberg, A. M.; Zhang, J. Z. *J. Phys. Chem. C* **2008**, *112*, 10323−10337.
(3) Mirkin, C. A.; Letsinger, R. L.; Mucic, R. C.; Storhoff, J. J. *Nature* **1996**, *382*, 607−609.
(4) Thaxton, C. S.; Georganopoulou, D. G.; Mirkin, C. A. *Clin. Chim. Acta* **2006**, *363*, 120−126.
(5) Baptista, P.; Pereira, E.; Eaton, P.; Doria, G.; Miranda, A.; Gomes, I.; Quaresma, P.; Franco, R. *Anal. Bioanal. Chem.* **2008**, *391*, 943−950.
(6) Mulvaney, P.; Giersig, M.; Henglein, A. J. *Phys. Chem.* **1993**, *97*, 7061−7064.
(7) Mulvaney, P. *Langmuir* **1996**, *12*, 788.
(8) Link, S.; Wang, Z. L.; El-Sayed, M. A. *J. Phys. Chem. B* **1999**, *103*, 3529−3533.
(9) Larguinho, M.; Baptista, P. V. *J. Proteomics* **2011**, [Epub ahead of print].
(10) Cao, Y.; Jin, R.; Mirkin, C. A. *J. Am. Chem. Soc.* **2001**, *123*, 7961−7962.
(11) Cao, Y.; Jin, R.; Thaxton, C. S.; Mirkin, C. A. *Talanta* **2005**, *67*, 449−455.
(12) Doria, G.; Larguinho, M.; Dias, J. T.; Pereira, E.; Franco, R.; Baptista, P. V. *Nanotechnology* **2010**, *21*, 255101.
(13) Sylvestre, J. P.; Kabashin, A. V.; Sacher, E.; Meunier, M.; Luong, J. H. T. *J. Am. Chem. Soc.* **2004**, *126*, 7176−7177.
(14) Besner, S.; Kabashin, A. V.; Winnik, F. M.; Meunier, M. *J. Phys. Chem. C* **2009**, *113*, 9526−9531.
(15) Petersen, S.; Barcikowski, S. *J. Phys. Chem. C* **2009**, *113*, 19830−19835.
(16) Liu, J.; Cao, Z.; Lu, Y. *Chem. Rev.* **2009**, *109*, 1948−1998.
(17) Kabashin, A. V.; Meunier, M. *J. Phys. Conf. Ser.* **2007**, *59*, 354−359.
(18) Besner, S.; Meunier, M. *J. Phys. Chem. C* **2010**, *114*, 10403−10409.
(19) Ramaswamy, S.; Musser, J. M. *Tubercle Lung Dis.* **1998**, *79*, 3−29.
(20) O'Sullivan, D. M.; McHugh, T. D.; Gillespie, S. H. *J. Antimicrob. Chemother.* **2005**, *55*, 674−679.
(21) Rachkov, A.; Patskovsky, S.; Soldatkin, A.; Meunier, M. *Talanta* **2011**, *85*, 2094−2099.
(22) Markham, N. R.; Zuker, M. *Nucleic Acids Res.* **2005**, *33*, 577−581.
(23) Teles, F. R. R.; Fonseca, L. P. *Talanta* **2008**, *77*, 606−623.
(24) Sambrook, J.; Fritsch, E. F.; Maniatis, T. *Molecular Cloning: A Laboratory Manual*, 2nd ed.; Cold Spring Harbor Laboratory Press: Cold Spring Harbor, NY, 1989; Vol. 2.
(25) Murphy, M. C.; Rasnik, I.; Cheng, W.; Lohman, T. M.; Ha, T. *Biophys. J.* **2004**, *86*, 2530−2537.
(26) Wormeester, H.; Kooij, E. S.; Poelsema, B. *Phys. Status Solidi A* **2008**, *205*, 756−763.
(27) Elhadj, S.; Singh, G.; Saraf, R. F. *Langmuir* **2004**, *20*, 5539−5543.
(28) Su, X.; Wu, Y. J.; Knoll, W. *Biosens. Bioelectron.* **2005**, *21*, 719−726.
(29) Tinland, B.; Pluen, A.; Sturm, J.; Weill, G. *Macromolecules* **1997**, *30*, 5763−5765.
(30) Mbindyo, J. K. N.; Reiss, B. D.; Martin, B. R.; Keating, C. D.; Natan, M. J.; Mallouk, T. E. *Adv. Mater.* **2001**, *13*, 249−254.
(31) Herne, T. M.; Tarlov, M. J. *J. Am. Chem. Soc.* **1997**, *119*, 8916−8920.
(32) Sylvestre, J. P.; Kabashin, A. V.; Sacher, E.; Meunier, M.; Luong, H. T. L. *J. Am. Chem. Soc.* **2004**, *126*, 7176−7177.
(33) Xu, Y-l.; Gustafson, B.Å.S. *J. Quant. Spectrosc. Radiat. Transfer* **2001**, *70*, 395−419.
(34) Li, F.; Li, J.; Wang, C.; Zhang, J.; Li, X.-F.; Le, X. C. *Anal. Chem.* **2011**, *83*, 6464−6467.
(35) Stoeva, S. I.; Lee, J. S.; Thaxton, C. S.; Mirkin, C. A. *Angew Chem., Int. Ed.* **2006**, *45*, 3303−3306.
(36) Hurst, S. J.; Lytton-Jean, A. K. R.; Mirkin, C. A. *Anal. Chem.* **2006**, *78*, 8313−8318.
(37) Ma, Y.; Chechik, V. *Langmuir* **2011**, *27*, 14432−14437.
(38) Bellino, M. G.; Calvo, E. J.; Gordillo, G. *Phys. Chem. Chem. Phys.* **2004**, *6*, 424−428.
(39) Petersen, S.; Barcikowski, S. *J. Phys. Chem. C* **2009**, *113*, 19830−19835.
(40) Zhong, Z. Y.; Patskovsky, S.; Bouvrette, P.; Luong, J. H. T.; Gendanken, A. *J. Phys. Chem. B* **2004**, *108*, 046−4052.
(41) Compagnini, G.; Messina, E.; Puglisi, O.; Nicolosi, V. *Appl. Surf. Sci.* **2007**, *254*, 1007−1011.